1D to 2D Self Assembly of Cyclic Peptides

Ignacio Insua & Javier Montenegro*

Centro Singular de Investigación en Química Biolóxica e Materiais Moleculares (CIQUS), Departamento de Química Orgánica, Universidade de Santiago de Compostela, 15782, Spain.

**e-mail: javier.montenegro@usc.es*

Table of contents

1. Materials

All reagents and solvents were purchased from Acros Organics, Aldrich, Fisher Scientific, Iris Biotech and Novabiochem. Dichloromethane was dried under reflux over calcium hydride. Glass slides for fluoresce microscopy were obtained from Ibidi (Cat# 80827). TEM grids (i. Cu carbon type-B, 300 mesh; ii. Holey carbon, 400 mesh) and PELCO® mica discs for AFM were purchased from Ted Pella.

2. Instrumentation

Peptide purification was carried out by preparative reverse-phase HPLC (Waters 1525 and 2489) using an Agilent Eclipse XDB-C18 column. ^{1}H-NMR spectra were acquired on Varian 300 or 500 MHz spectrometers at 298K; chemical shifts (δ) are reported in ppm relative to that of DMSO (δ = 2.50 ppm). Analytical UHPLC of the peptide was performed on an Agilent 1260 Infinity II fitted with an Agilent SB-C18 column and connected to a 6120 quadrupole MS detector. HR-MS was acquired on a Bruker MicroTOF. FT-IR spectra were acquired on a PerkinElmer Spectrum II fitted with an ATR. Epifluorescence micrographs were taken with a Nikon Eclipse T*i* (60x immersion objective, FITC cube: Ex=475/35 nm; Em=530/43 nm). STEM images were acquired on a FESEM Ultra plus (Zeiss) operating at 20 kV from unstained samples. Non-contact mode AFM analysis was performed on a NX-10 instrument fitted with ACTA 10M cantilevers (Park systems). Cross-polarised microscopy was performed on an Olympus BX51 fitted with two rotary polarisers. Wide-angle X-ray scattering (WAXS) was measured on a Bruker D8 VENTURE PHOTON-III 14 κ-geometry diffractometer fitted with an Incoatec IμS 3.0 microfocus sealed tube (Cu Kα, λ = 1.54178 Å) and a multilayer mirror monochromator. Circular dichroism spectra were recorded on a Jasco J-1100 CD spectrometer from a 2 mm quartz cuvette. Fluorescence spectra were acquired on a Varian Cary Eclipse from a 1 cm quartz cuvette. Dynamic light scattering (DLS) data was acquired on a Zetasizer Nano ZSP (Malvern).

3. Abbreviations

AcCN: acetonitrile; DCM: dichloromethane; DIPEA: *N*,*N*-diisopropylethylamine; DMF: *N*,*N*-dimethylformamide; DMSO: dimethyl sulfoxide; FITC: fluorescein isothiocyanate; Fmoc: 9-fluorenylmethyloxycarbonyl; HBTU: *N*,*N*,*N*′,*N*′-tetramethyl-*O*-(1*H*-benzotriazol-1-yl)uranium hexafluorophosphate; PyAOP: (7-azabenzotriazol-1-yloxy)trispyrrolidinophosphonium hexafluorophosphate; TFA: trifluoroacetic acid, ThT: thioflavin-T, TIPS: triisopropylsilane, Trt: trityl.

4. Synthesis and purification of cyclic peptides

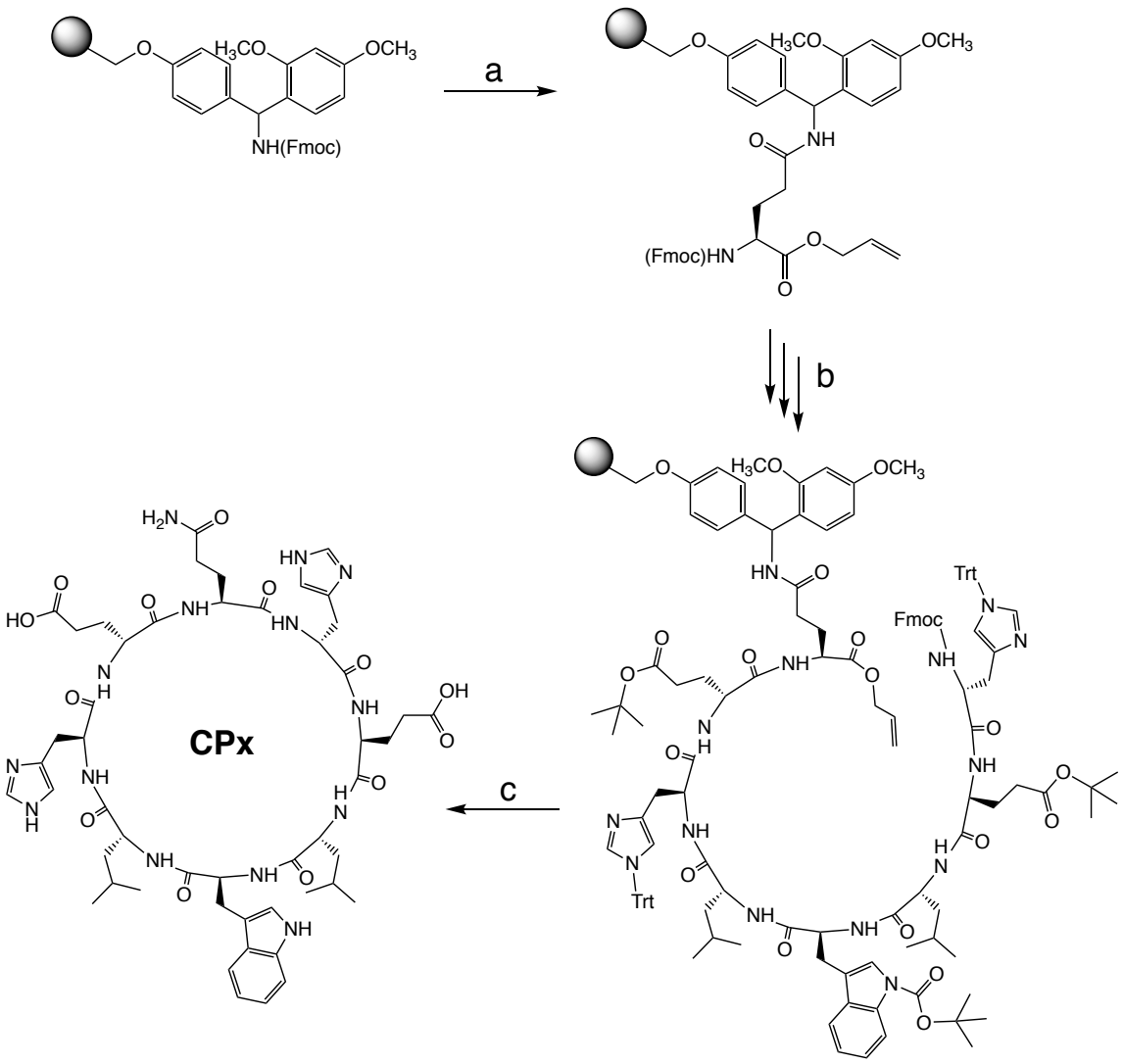

Scheme S1 a) *Rink amide resin functionalisation*: i) Piperidine 20% v/v in DMF, 30 min; ii) Fmoc-L-Glu-OAll, HBTU, DIPEA, DMF, 1h. **b)** *Peptide elongation*: i) Piperidine 20% v/v in DMF, 15 min; ii) amino acid, HBTU, DIPEA, DMF, 30 min; Repeat 7 cycles with the corresponding amino acids. **c)** i) *OAllyl removal*: $Pd(OAc)_2$, PPh_3, phenylsilane, 4-methylmorpholine, DCM, overnight; ii) *Fmoc removal*: Piperidine 20% v/v in DMF, 30 min; iii) *Peptide cyclisation*: PyAOP, DIPEA, DMF, overnight; iv) *Peptide cleavage from the resin*: TFA, DCM, H_2O, TIPS, 2h.

Detailed synthetic protocol:

Fmoc-Rink amide SPPS resin (135.0 mg, 0.1 mmol) was swollen in DMF for 30 min and the Fmoc group removed by treatment with piperidine 20% v/v in DMF (2 mL) for 30 min. The resin was then washed and treated with Fmoc-L-Glu(OH)-OAll (163.6 mg, 0.4 mmol), HBTU (151.5 mg, 0.4 mmol) and DIPEA (105 µL, 0.6 mmol) in DMF (2 mL) for 1 h. After this time, we followed cycles of Fmoc removal (2 mL of piperidine 20% v/v in DMF for 15 min) and amino acid coupling (0.4 mmol of amino acid, 0.4 mmol of HBTU, 0.6 mmol of DIPEA in 2 mL of DMF for 30 min) until all amino acids were coupled, leaving the *N*-terminal Fmoc group still on the peptide.

For OAllyl removal, the resin was thoroughly washed with DMF and DCM, and then reacted with 2 mL of a pre-mixed cocktail of $Pd(OAc)_2$ (6.7 mg, 0.03 mmol), PPh_3 (39.3 mg, 0.15 mmol), 4-methylmorpholine (110 µL, 1.0 mmol) and phenylsilane (123 µL, 1.0 mmol) in dry DCM overnight. The resin was then filtered and washed with DCM, 10 mL of DIPEA 2% v/v in DMF, DMF, and then twice with 2 mL of 0.5% m/m diethyldithiocarbamate in DMF for 30 min to remove all traces of Pd.

For *N*-terminal Fmoc removal, the resin was reacted with 2 mL of piperidine 20% v/v in DMF for 30 min and then washed with DMF.

The peptide was then cyclised by reacting the resin with PyAOP (208.4 mg, 0.4 mmol) and DIPEA (105 µL, 0.6 mmol) in 2 mL of DMF for 2 hours. This step was repeated twice more.

Once cyclised, the resin was washed with DMF and DCM, and the peptide was cleaved from the resin by treatment with 2 mL of TFA (90% v/v), DCM (5% v/v), H_2O (2.5% v/v) and TIPS (2.5% v/v) for 2 h. After this time, the acidic solution was filtered and concentrated under a flow of nitrogen, to be then precipitated into 45 mL of chilled diethyl ether. The suspension thus obtained was centrifuged (3 krcf, 10 min) and the pellet dissolved in a 1:1 mixture of H_2O:AcCN and purified by preparative reverse-phase HPLC (A = H_2O + 0.1% v/v TFA; B = AcCN + 0.1% v/v TFA; 15 mL·min^{-1}): 0 min (0% B) → 5 min (0% B) → 30 min (75% B) → 35 min (95% B) → 40 min (95% B); R_t = 19.9 min. Peptide fractions were concentrated *in vacuo* to remove TFA and AcCN, and the remaining aqueous solution was freeze dried.

A white powder was thus obtained: **CPx** (30 mg; 28% yield), **CPxAla** (15 mg; 15% yield), **CPx-Glu** (37 mg; 35% yield) and **CPx-His** (22 mg; 21% yield).

5. CPx characterisation

5.1. ^{1}H-NMR (300 MHz, DMSO-*d*$_6$) δ = 0.64-1.31 (m, 18H, Leu *i*-Bu x2), 1.55-2.12 (m, 12H, Glu -C$\underline{H}_2$- x2 + Gln -C$\underline{H}_2$-), 2.80-3.11 (m, 6H, His -C$\underline{H}_2$- x2 + Trp -C$\underline{H}_2$-), 4.27-4.49 (m, 5H, Hα), 4.62-4.85 (m, 3H, Hα), 6.76 (s, 1H, Gln-CONH$_2$), 6.93 (t, *J* = 7.3 Hz, 1H, Trp), 7.02 (t, *J* = 7.3 Hz, 1H, Trp), 7.11 (d, *J* = 2.4 Hz, 1H, Trp), 7.22 (s, 1H, Gln-CONH$_2$), 7.28 (d, *J* = 8.1 Hz, 1H, Trp), 7.33 (d, *J* = 13.5 Hz, 2H, His x2), 7.68 (d, *J* = 7.8 Hz, 1H, Trp), 8.04 (d, *J* = 8.7 Hz, 1H, CONH), 8.10 (d, *J* = 8.3 Hz, 1H, CONH), 8.17 (d, *J* = 8.2 Hz, 1H, CONH), 8.26 (d, *J* = 7.9 Hz, 1H, CONH), 8.32 (d, *J* = 8.3 Hz, 1H, CONH), 8.38 (d, *J* = 8.3 Hz, 1H, CONH), 8.40 (d, *J* = 8.2 Hz, 1H, CONH), 8.46 (d, *J* = 8.7 Hz, 1H, CONH), 8.96 (dd, *J* = 11.9, 1.3 Hz, 2H, His x2), 10.79 (d, *J* = 2.2 Hz, 1H, Trp-NH) ppm.

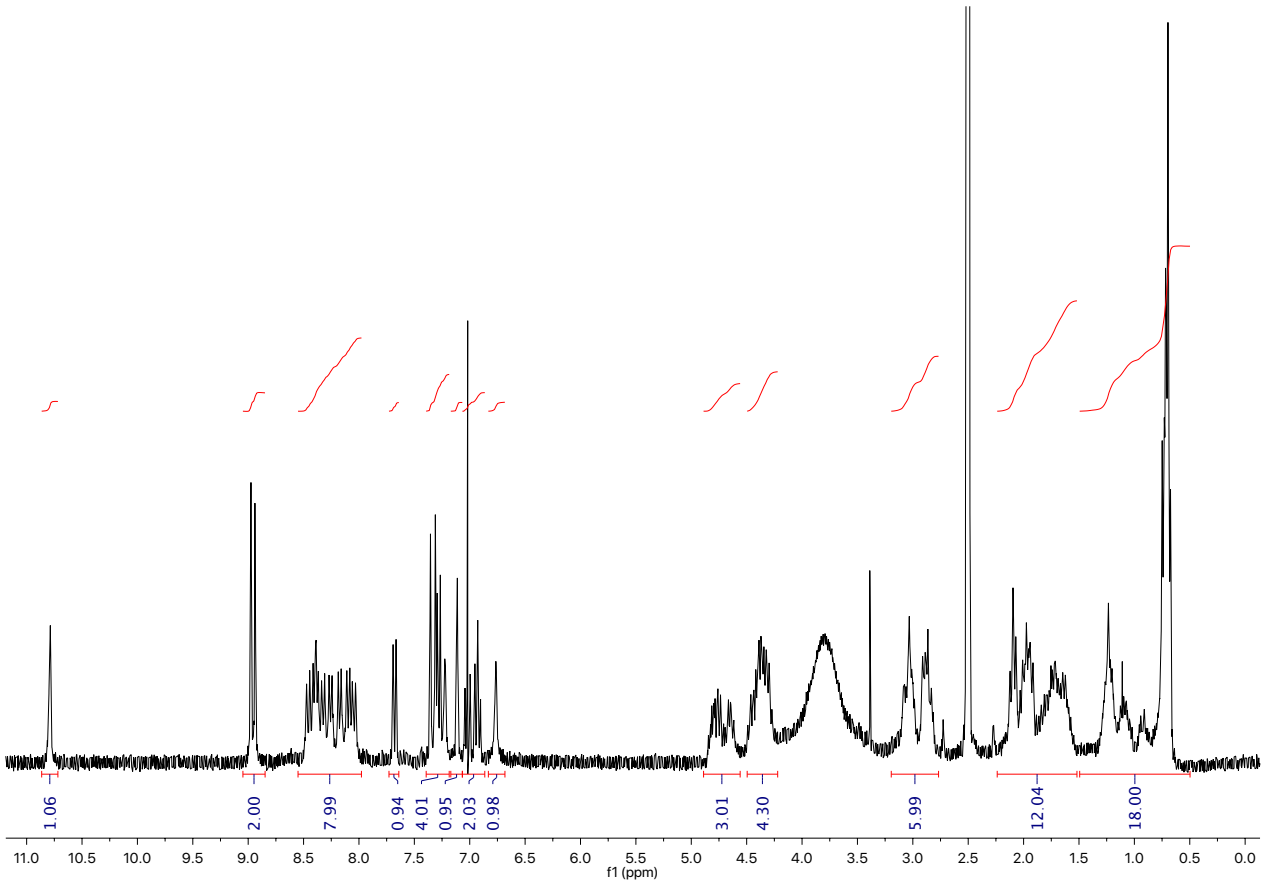

Figure S1 ^{1}H-NMR spectrum (300 MHz, DMSO-*d*$_6$) of **CPx**.

5.2. UHPLC-MS (C18-ESI, +eV) A = H_2O + 0.1% v/v TFA; B = AcCN + 0.1% v/v TFA; 0.35 mL·min^{-1}: 0 min (0% B) → 2 min (0% B) → 21 min (75% B) → 22 min (95% B); R_t = 12.5 min. m/z = 1,073.4 ([M+H]$^+$), 537.3 ([M+2H]$^{2+}$).

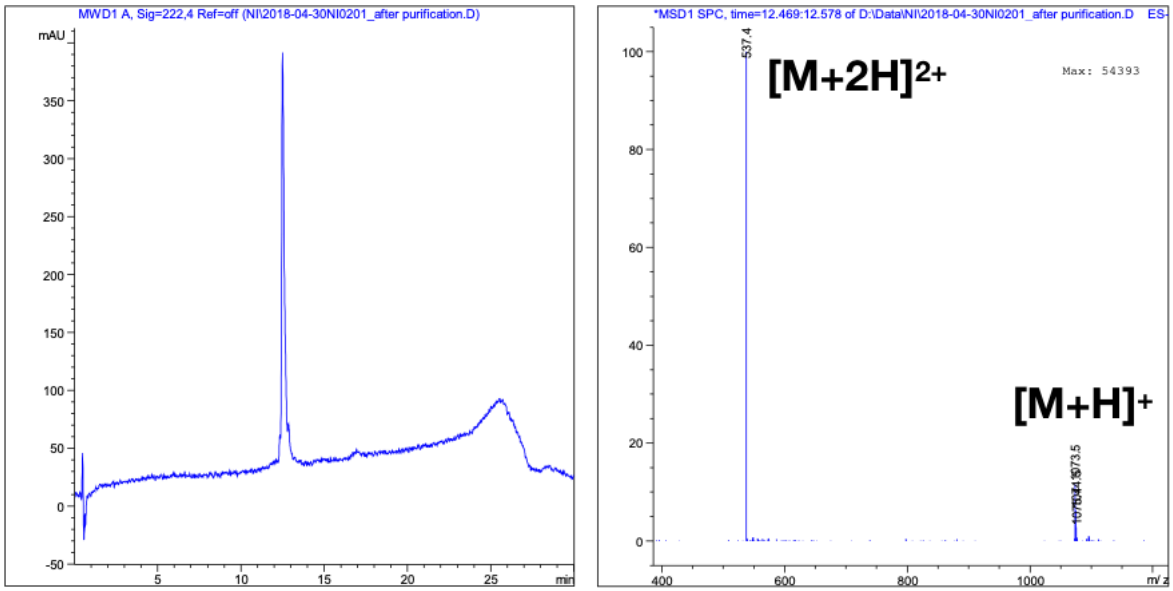

Figure S2 Reverse-phase UHPLC (left) and mass spectrum of the peak in the chromatogram (right) of **CPx**.

5.3. HR-MS (ESI, +eV) m/z = 1073.5163 (calculated for [M+H]$^+$) 1073.5162 (found).

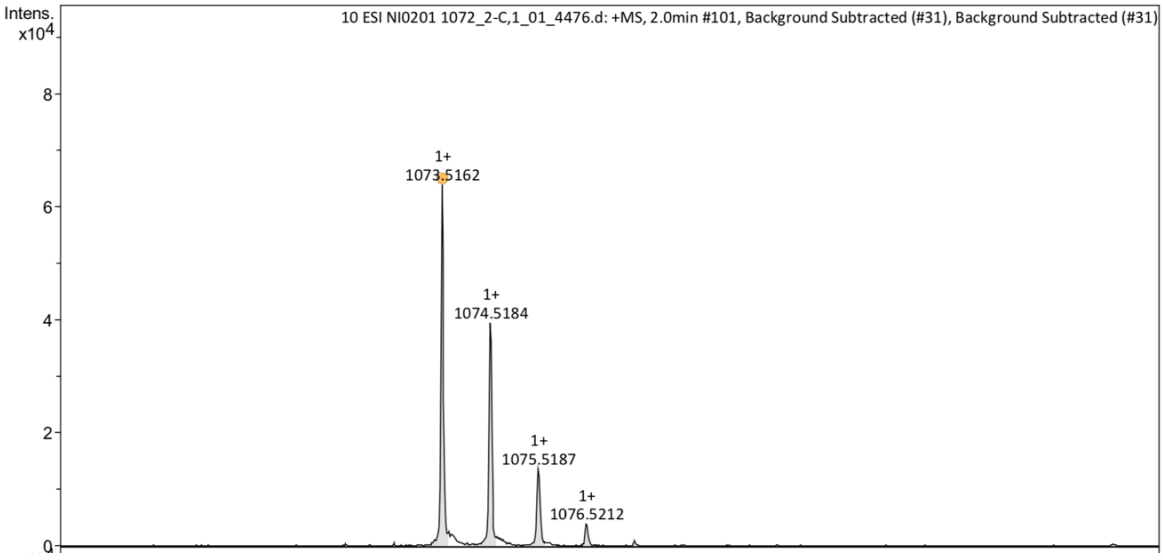

Figure S3 High resolution mass spectrometry (HR-MS) analysis of **CPx**.

6. CPxAla characterisation

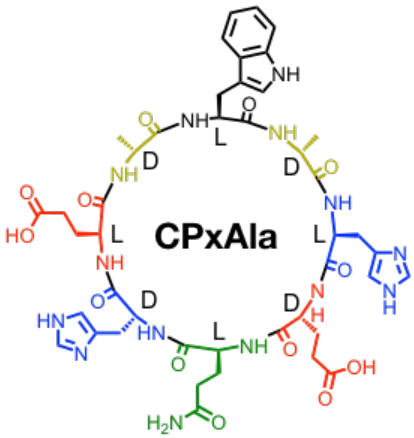

6.1. ^{1}H-NMR (300 MHz, DMSO-*d*$_6$) δ = 0.94 (t, *J* = 6.6 Hz, 6H, Ala x2), 1.56-2.12 (m, 12H, Glu -C<u>H</u>$_2$- x2 + Gln -C<u>H</u>$_2$-), 2.80-3.09 (m, 6H, His -C<u>H</u>$_2$- x2 + Trp -C<u>H</u>$_2$-), 4.25-4.45 (m, 5H, Hα), 4.52-4.60 (m, 1H, Hα), 4.69-4.79 (m, 2H, Hα), 6.77 (s, 1H, Gln-CONH$_2$), 6.94 (t, *J* = 7.4 Hz, 1H, Trp), 7.03 (t, *J* = 7.3 Hz, 1H, Trp), 7.12 (d, *J* = 2.3 Hz, 1H, Trp), 7.22 (s, 1H, Gln-CONH$_2$), 7.29 (d, *J* = 7.7 Hz, 1H, Trp), 7.32 (d, *J* = 12.7 Hz, 2H, His x2), 7.62 (d, *J* = 7.7 Hz, 1H, Trp), 8.11 (d, *J* = 8.3 Hz, 2H, CONH), 8.17 (d, *J* = 8.3 Hz, 1H, CONH), 8.24-8.31 (m, 4H, CONH), 8.43 (d, *J* = 8.4 Hz, 1H, CONH), 8.95 (d, *J* = 5.4 Hz, 2H, His x2), 10.78 (s, 1H, Trp-NH) ppm.

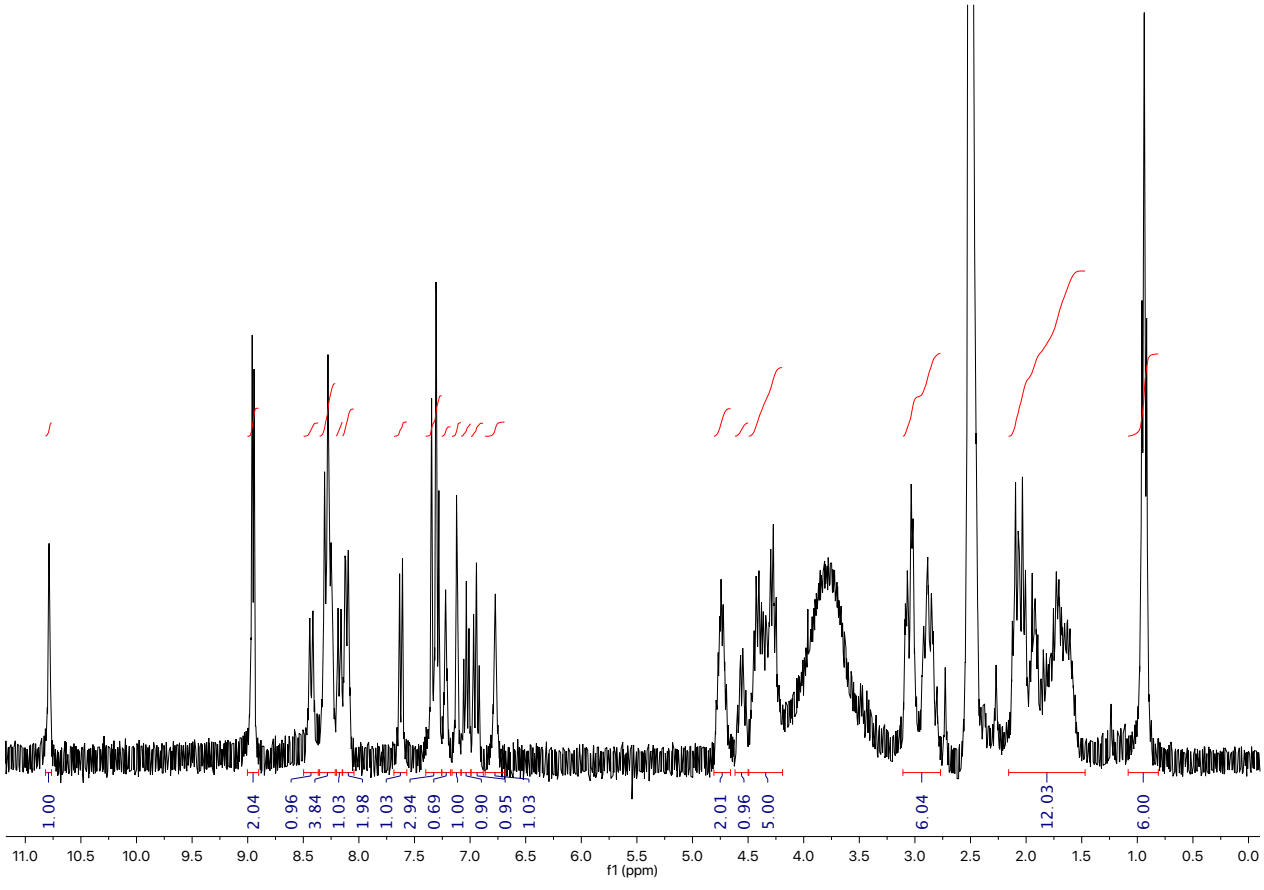

Figure S4 ^{1}H-NMR spectrum (300 MHz, DMSO-*d*$_6$) of **CPxAla**.

6.2. UHPLC-MS (C18-ESI, +eV) A = H_2O + 0.1% v/v TFA; B = AcCN + 0.1% v/v TFA; 0.35 mL·min^{-1}: 0 min (0% B) → 2 min (0% B) → 21 min (75% B) → 22 min (95% B); R_t = 9.9 min. m/z = 989.4 ([M+H]$^+$), 495.4 ([M+2H]$^{2+}$).

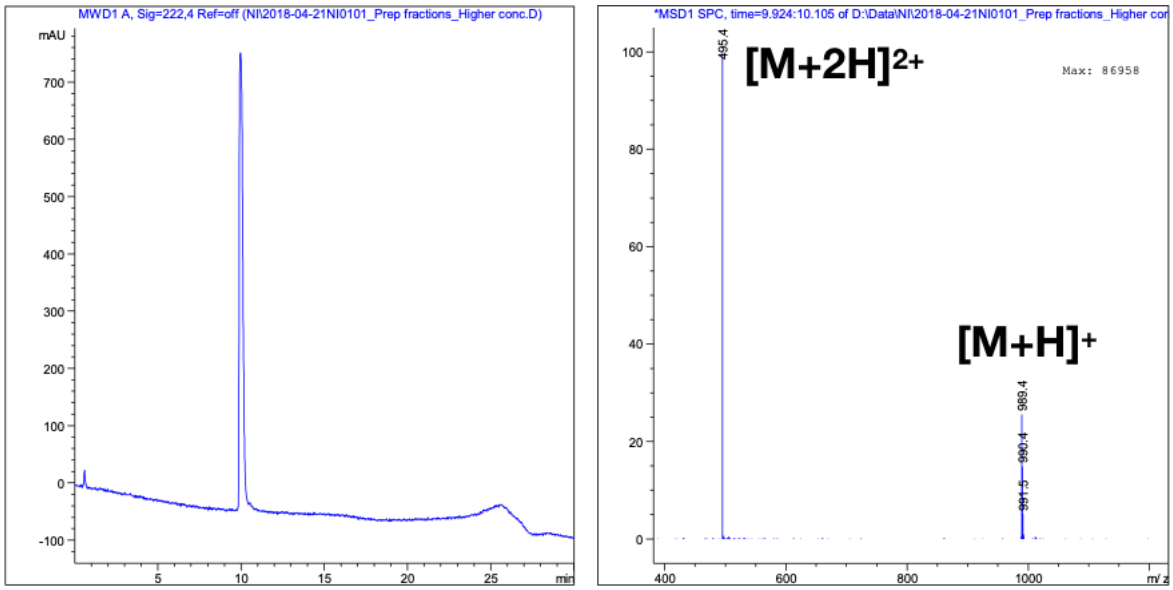

Figure S5 Reverse-phase UHPLC (left) and mass spectrum of the peak in the chromatogram (right) of **CPxAla**.

6.3. HR-MS (ESI, +eV) m/z = 989.4224 (calculated for [M+H]$^+$) 989.4228 (found).

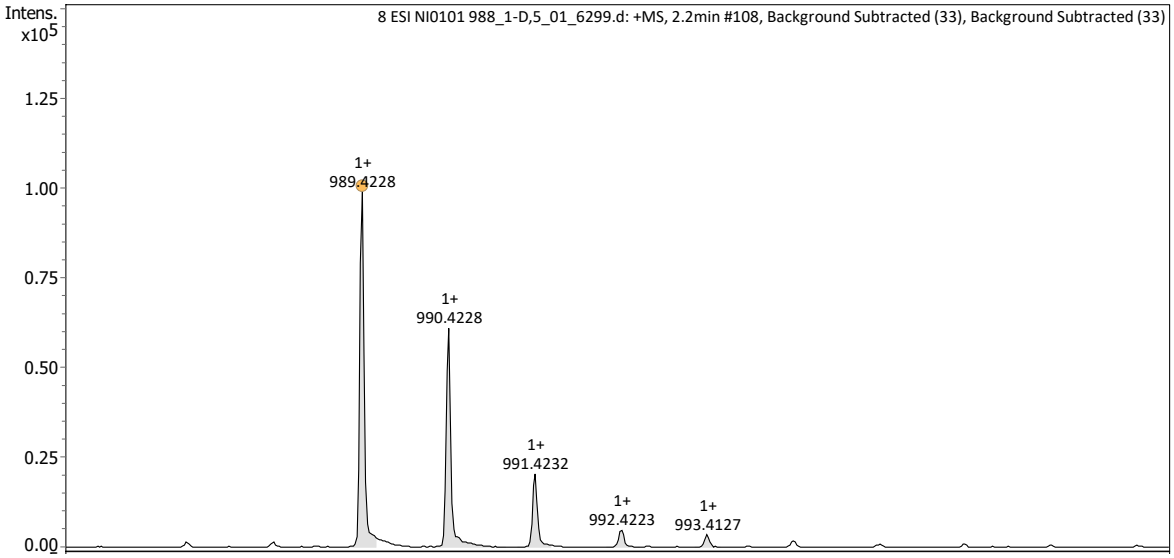

Figure S6 High resolution mass spectrometry (HR-MS) analysis of **CPxAla**.

7. CPx-Glu characterisation

7.1. ^{1}H-NMR (500 MHz, DMSO-*d*$_6$) δ = 0.69-1.26 (m, 18H, Leu *i*-Bu x2), 1.58-2.11 (m, 12H, Gln -C<u>H</u>$_2$- x3), 2.84-3.11 (m, 6H, His -C<u>H</u>$_2$- x2 + Trp -C<u>H</u>$_2$-), 4.20-4.44 (m, 5H, Hα), 4.62-4.81 (m, 3H, Hα), 6.74 (s, 1H, Gln-CONH$_2$), 6.80 (s, 2H, Gln-CONH$_2$ x2), 6.93 (t, *J* = 7.7 Hz, 1H, Trp), 7.01 (t, *J* = 8.0 Hz, 1H, Trp), 7.11 (d, *J* = 2.7 Hz, 1H, Trp), 7.22 (s, 2H, Gln-CONH$_2$ x2), 7.24 (s, 1H, Gln-CONH$_2$), 7.28 (d, *J* = 8.0 Hz, 1H, Trp), 7.32 (d, *J* = 16.8 Hz, 2H, His x2), 7.66 (d, *J* = 7.9 Hz, 1H, Trp), 8.01 (d, *J* = 8.5 Hz, 1H, CONH), 8.09 (d, *J* = 8.4 Hz, 1H, CONH), 8.15 (d, *J* = 8.3 Hz, 1H, CONH), 8.28 (d, *J* = 8.6 Hz, 1H, CONH), 8.29 (d, *J* = 8.3 Hz, 1H, CONH), 8.33 (d, *J* = 8.5 Hz, 1H, CONH), 8.37 (d, *J* = 8.0 Hz, 1H, CONH), 8.47 (d, *J* = 8.7 Hz, 1H, CONH), 8.95 (dd, *J* = 18.5, 1.3 Hz, 2H, His x2), 10.79 (s, 1H, Trp-NH) ppm.

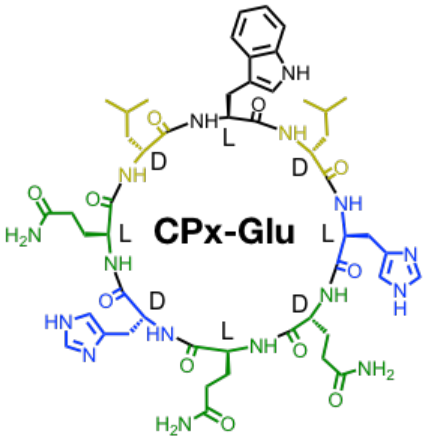

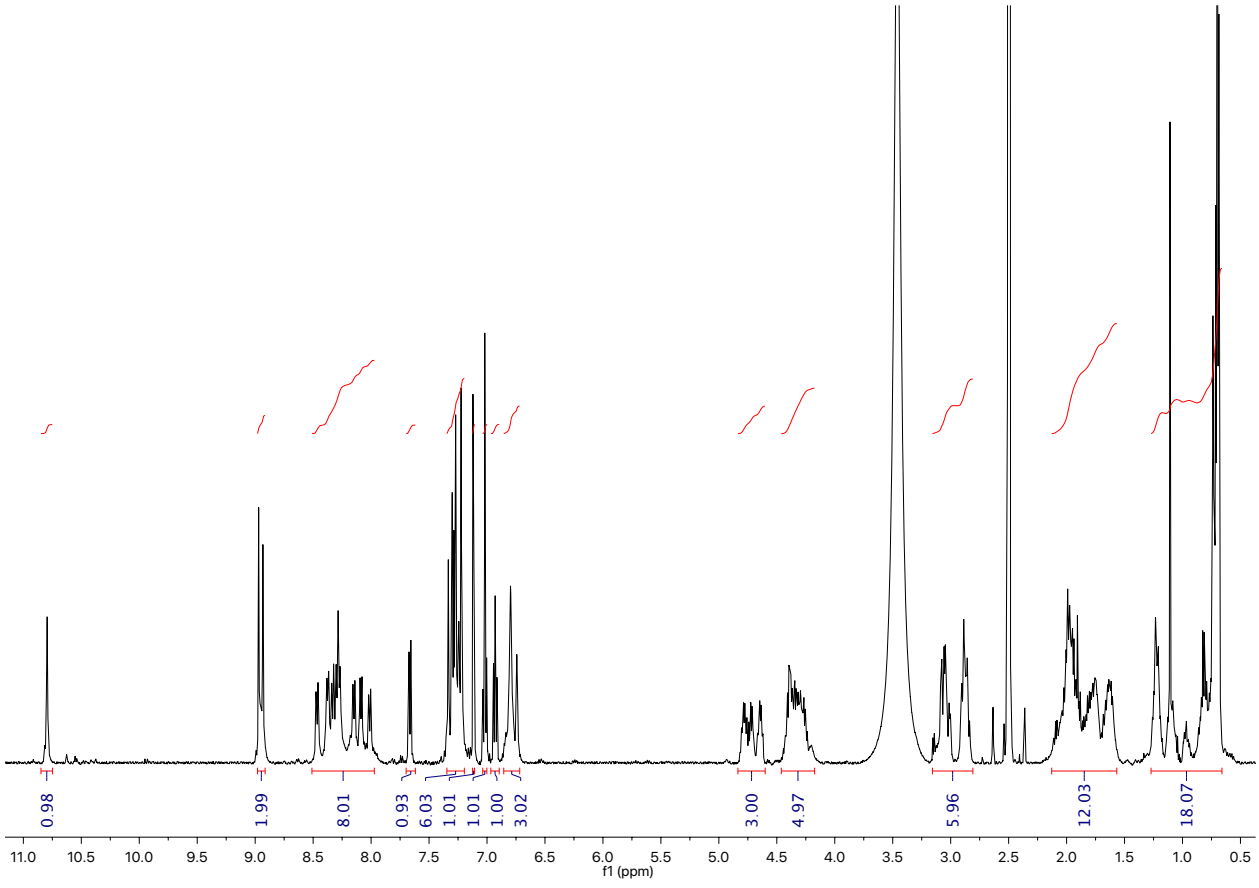

Figure S7 ^{1}H-NMR spectrum (500 MHz, DMSO-*d*$_6$) of **CPx-Glu**.

7.2. UHPLC-MS (C18-ESI, +eV) A = H_2O + 0.1% v/v TFA; B = AcCN + 0.1% v/v TFA; 0.35 mL·min^{-1}: 0 min (0% B) → 2 min (0% B) → 21 min (75% B) → 22 min (95% B); R_t = 11.9 min. m/z = 1071.6 ([M+H]$^+$), 536.4 ([M+2H]$^{2+}$).

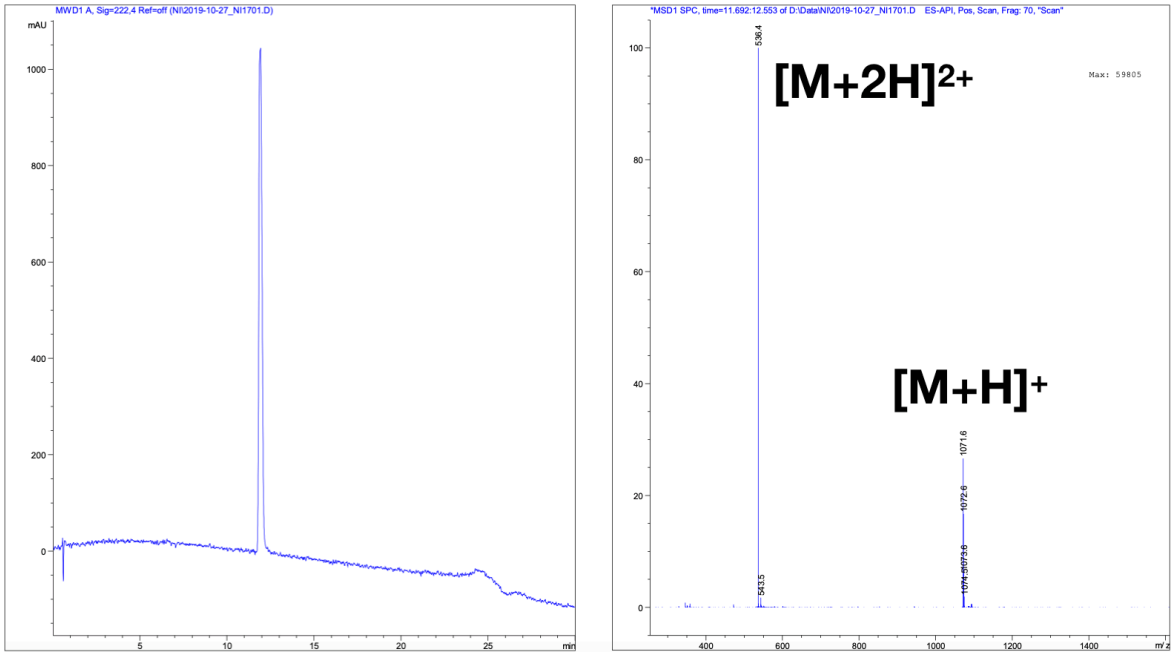

Figure S8 Reverse-phase UHPLC (left) and mass spectrum of the peak in the chromatogram (right) of **CPx-Glu**.

6.3. HR-MS (ESI, +eV) m/z = 1071.5483 (calculated for [M+H]$^+$) 1071.5481 (found).

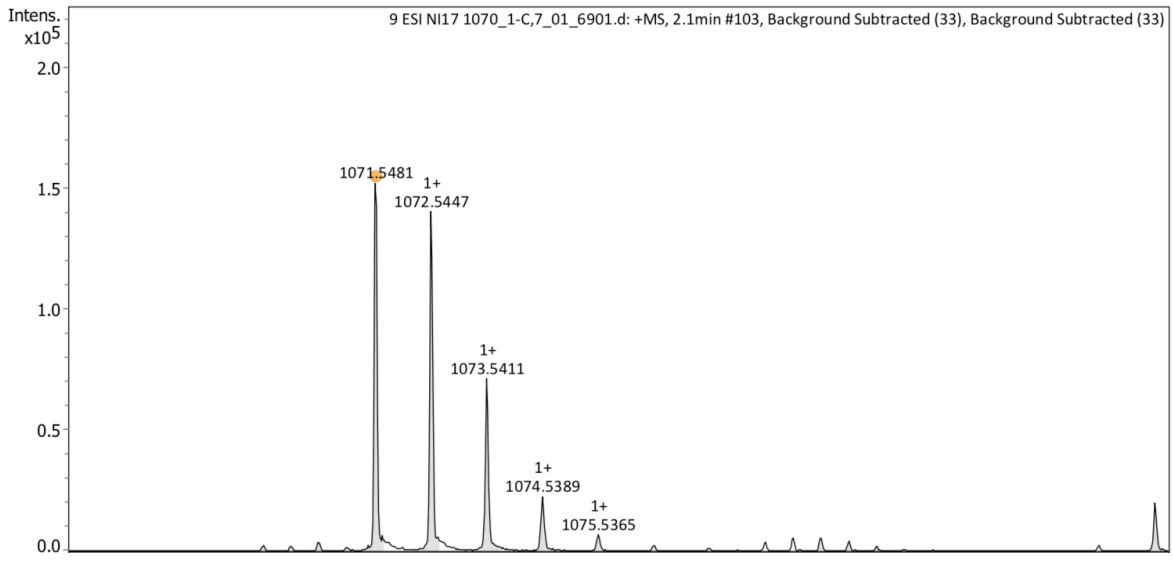

Figure S9 High resolution mass spectrometry (HR-MS) analysis of **CPx-Glu**.

8. CPx-His characterisation

8.1. ^{1}H-NMR (500 MHz, DMSO-*d_6:TFA [8:1]*) δ = 0.69-0.88 (m, 12H, Leu -CH_3 x4), 1.33 -1.56 (m, 6H, Leu -CH_2CH- x2), 1.73-2.24 (m, 20H, Gln + Glu -$(CH_2)_2$- x5), 2.90-3.16 (m, 2H, Trp -$C\underline{H}_2$-), 4.06-4.72 (m, 8H, Hα), 6.93 (t, *J* = 7.9 Hz, 1H, Trp), 6.99-7.03 (m, 1H, Trp), 7.13 (d, *J* = 15.6 Hz, 1H, Trp), 7.28 (d, *J* = 8.5 Hz, 1H, Trp), 7.66 (t, *J* = 9.5 Hz, 1H, Trp), 7.91-8.44 (m, 8H, CONH), 10.74 (s, 1H, Trp-NH) ppm.

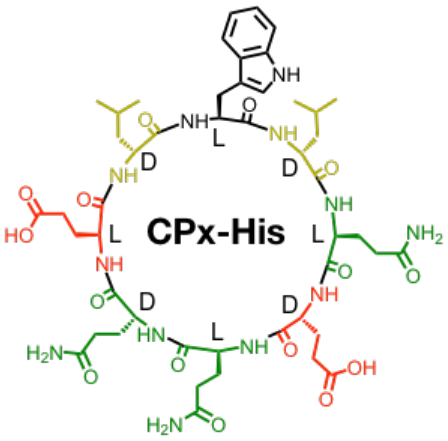

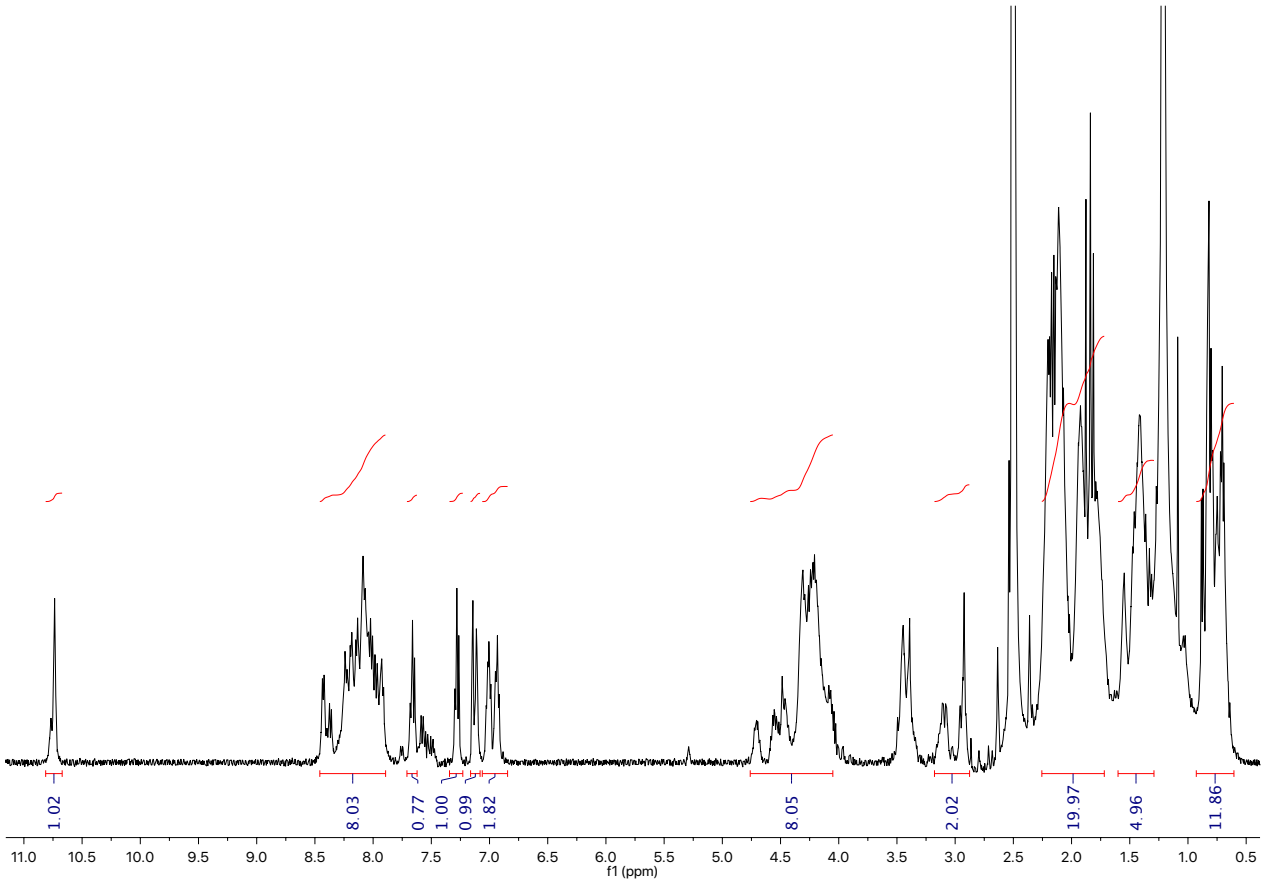

Figure S10 ^{1}H-NMR spectrum (500 MHz, DMSO-*d_6:TFA [8:1]*) of **CPx-His**.

8.2. UHPLC-MS (C18-ESI, +eV) A = H_2O + 0.1% v/v TFA; B = AcCN + 0.1% v/v TFA; 0.35 mL·min^{-1}: 0 min (0% B) → 2 min (0% B) → 21 min (75% B) → 22 min (95% B); R_t = 12.9 min. m/z = 1055.6 ([M+H]$^+$), 528.4 ([M+2H]$^{2+}$).

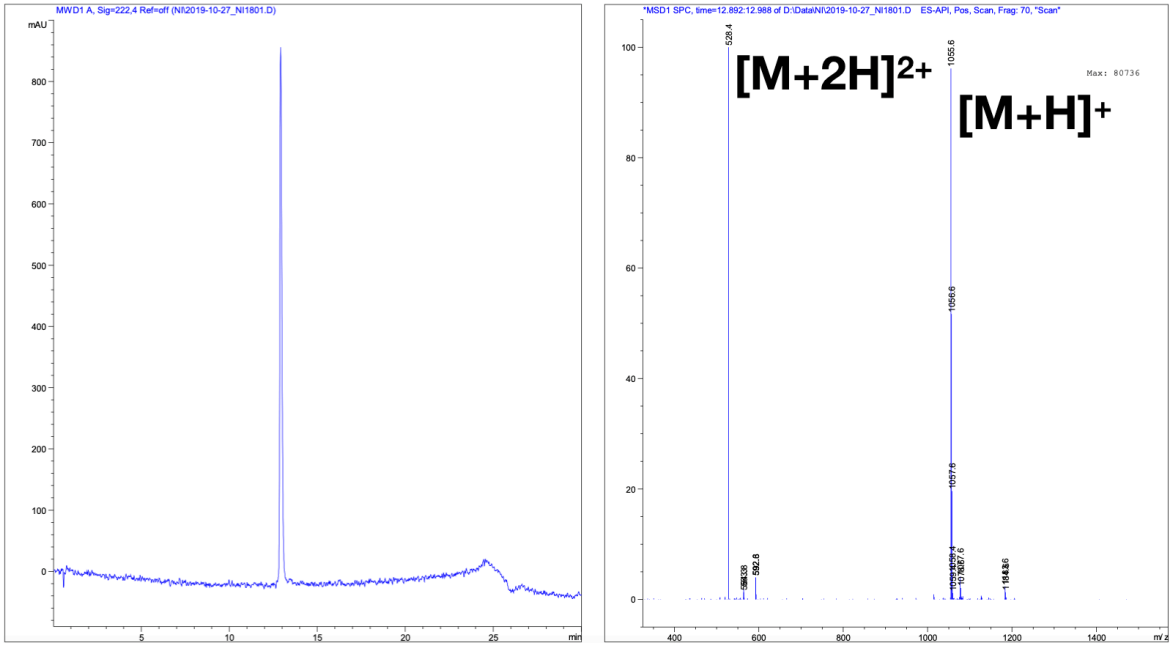

Figure S11 Reverse-phase UHPLC (left) and mass spectrum of the peak in the chromatogram (right) of **CPx-His**.

6.3. HR-MS (ESI, +eV) m/z = 1055.5156 (calculated for [M+H]$^+$) 1055.5153 (found).

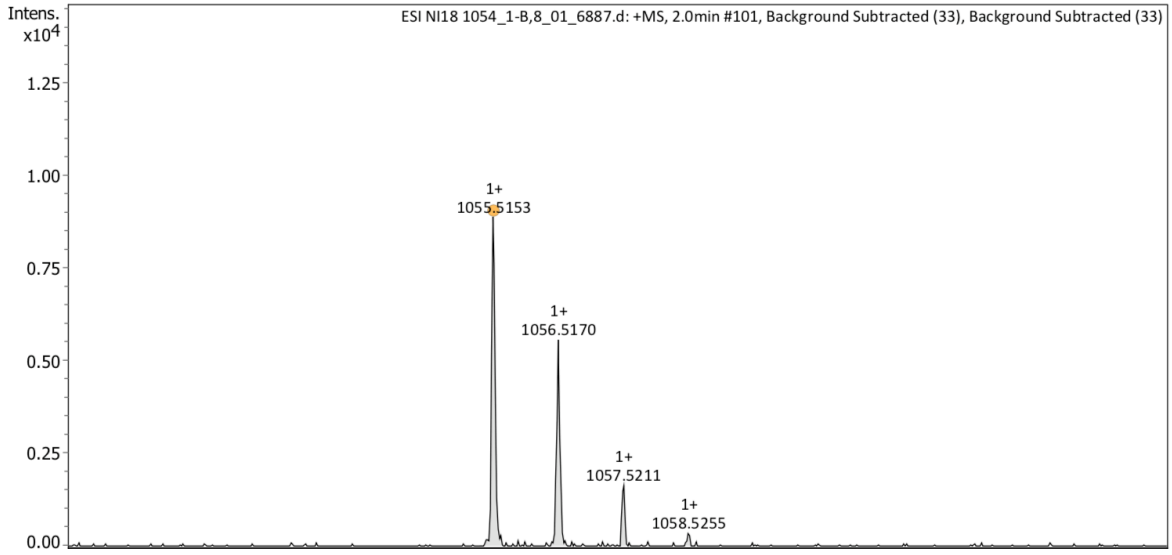

Figure S12 High resolution mass spectrometry (HR-MS) analysis of **CPx-His**.

9. Epifluorescence microscopy of CPx nanosheets

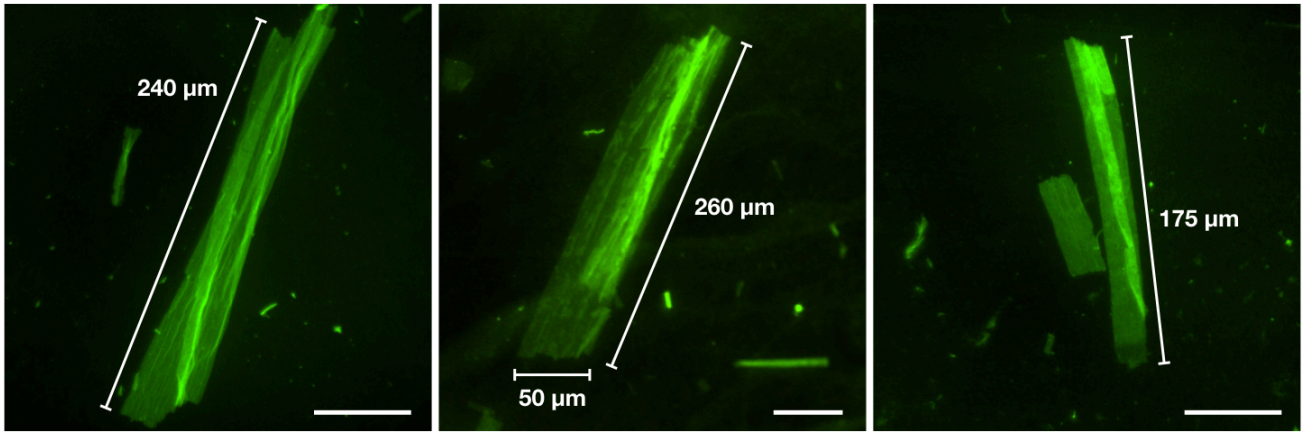

Figure S13 Epifluorescence micrographs of **CPx** nanosheets. Scale bars = 50 µm.

10. Scanning-transmission electron microscopy (STEM) of CPx nanosheets

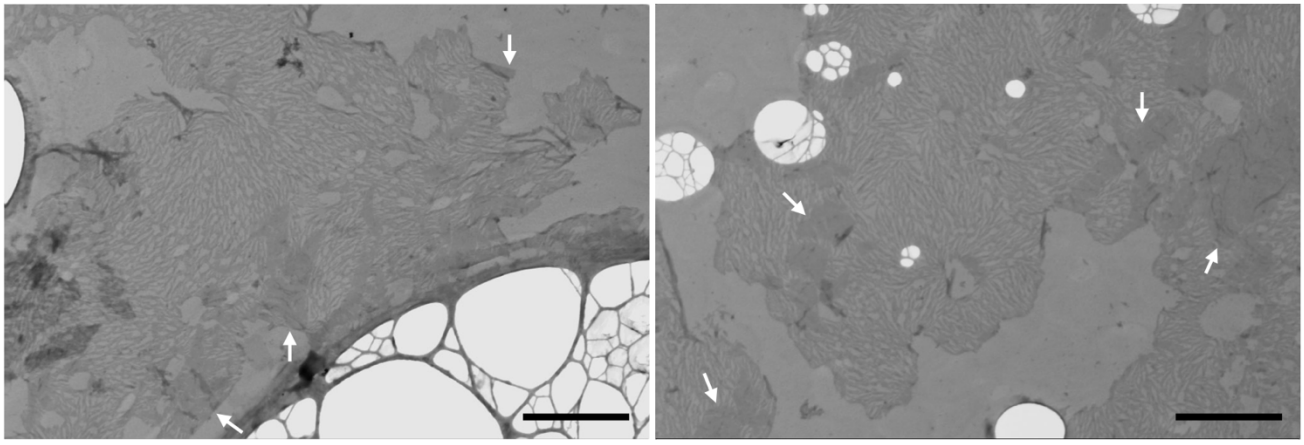

Figure S14 Scanning-transmission electron microscopy (STEM) of damaged **CPx** nanosheets. Aligned nanotubes can be found only on defined areas of the grid next to remaining sheet fragments (see arrows), suggesting the disassembly of sheets into their tubular building blocks. Scale bars = 1 µm.

11. Sonication of CPx nanosheets: Epifluorescence and electron microscopy

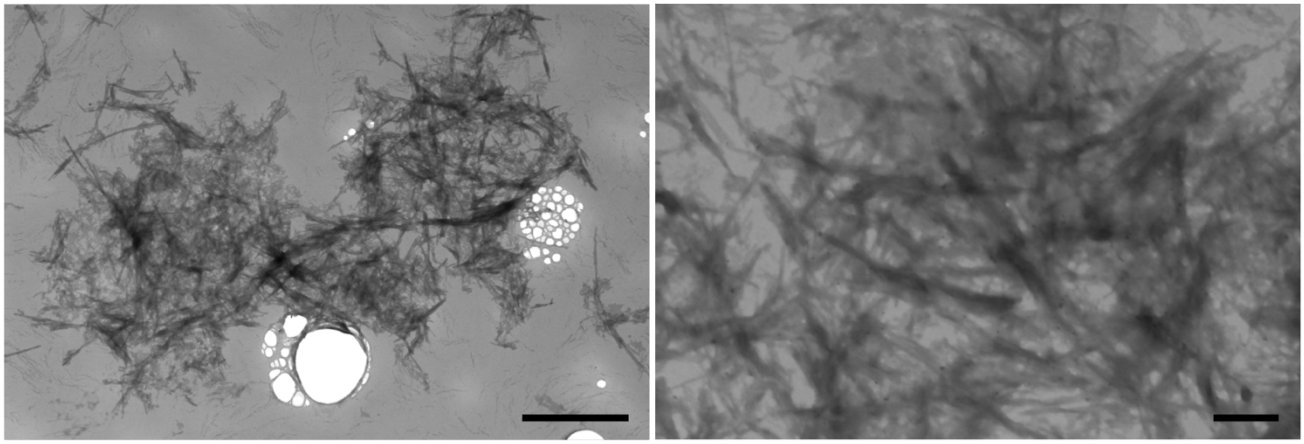

Figure S15 Scanning-transmission electron microscopy (STEM) of sonicated **CPx** nanosheets revealing their constituting nanotubes. Scale bars = 1 µm (left) and 200 nm (right).

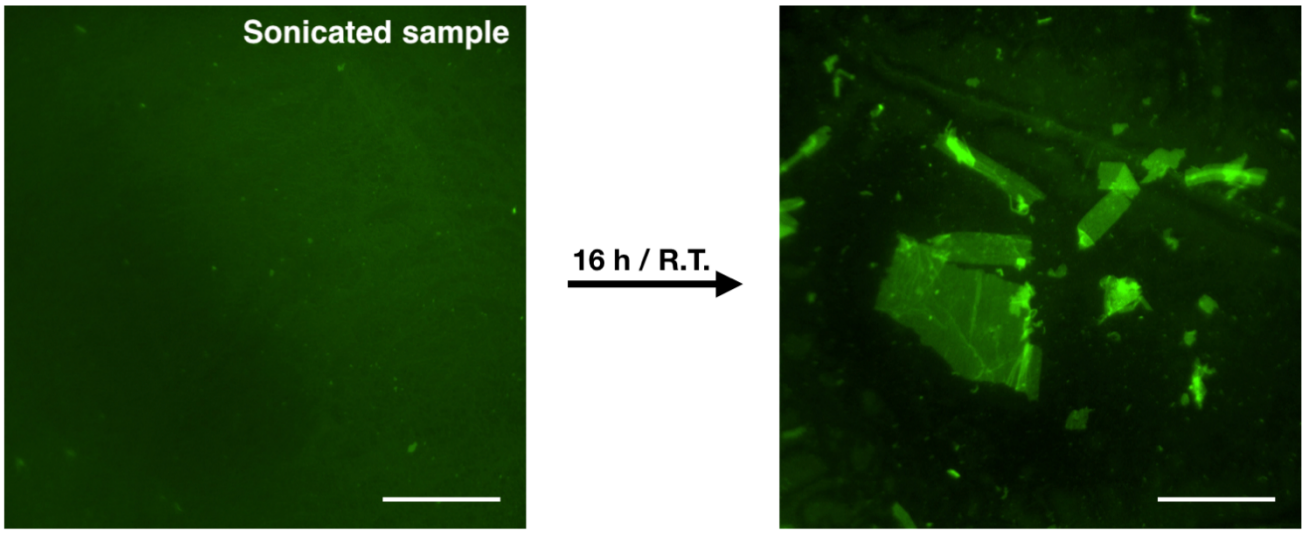

Figure S16 Epifluorescence micrographs of **CPx** nanosheets after sonication (left) and that same sample after 16 h (*i.e.* overnight) of recovery at room temperature (R.T.). Scale bars = 50 µm.

12. Annealing of CPx nanosheets: Electron microscopy

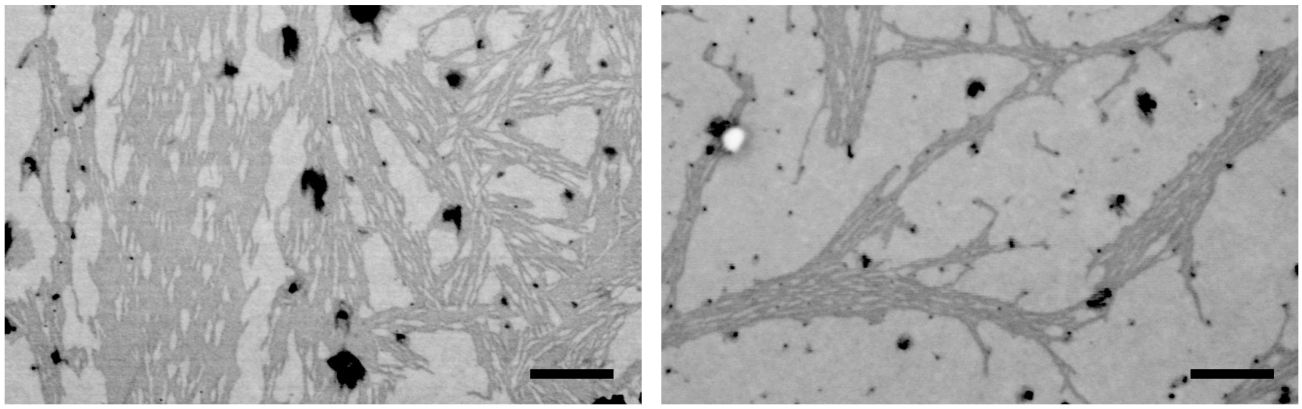

Figure S17 Scanning-transmission electron microscopy (STEM) of **CPx** samples (100 µM) heated at 80°C for 1.5 h. Scale bars = 300 nm.

13. Annealing of CPx nanosheets: Dynamic light scattering (DLS)

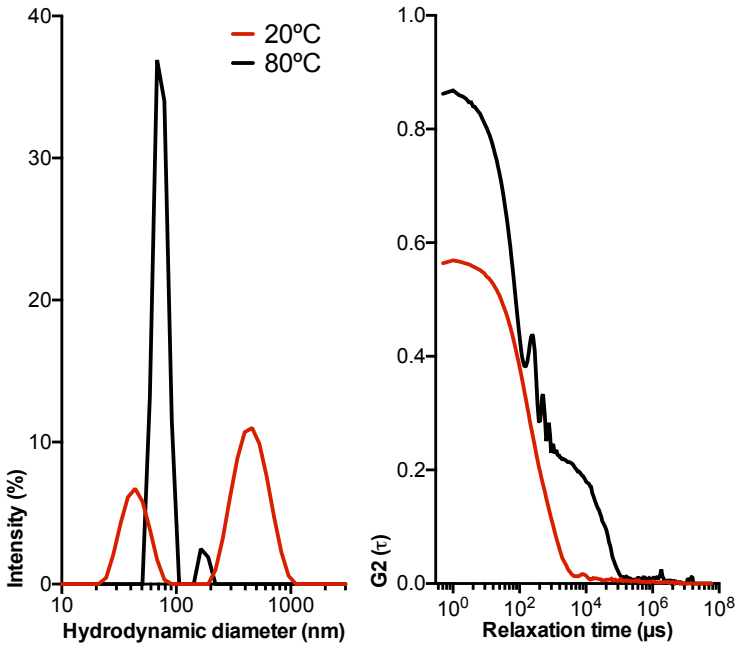

Figure S18 Dynamic light scattering (DLS) characterisation of **CPx** samples (100 µM) at 80°C and 20°C. Left: Size-Intensity plot. Right: Correlograms.

14. Exploration of self-assembling conditions of CPx nanosheets

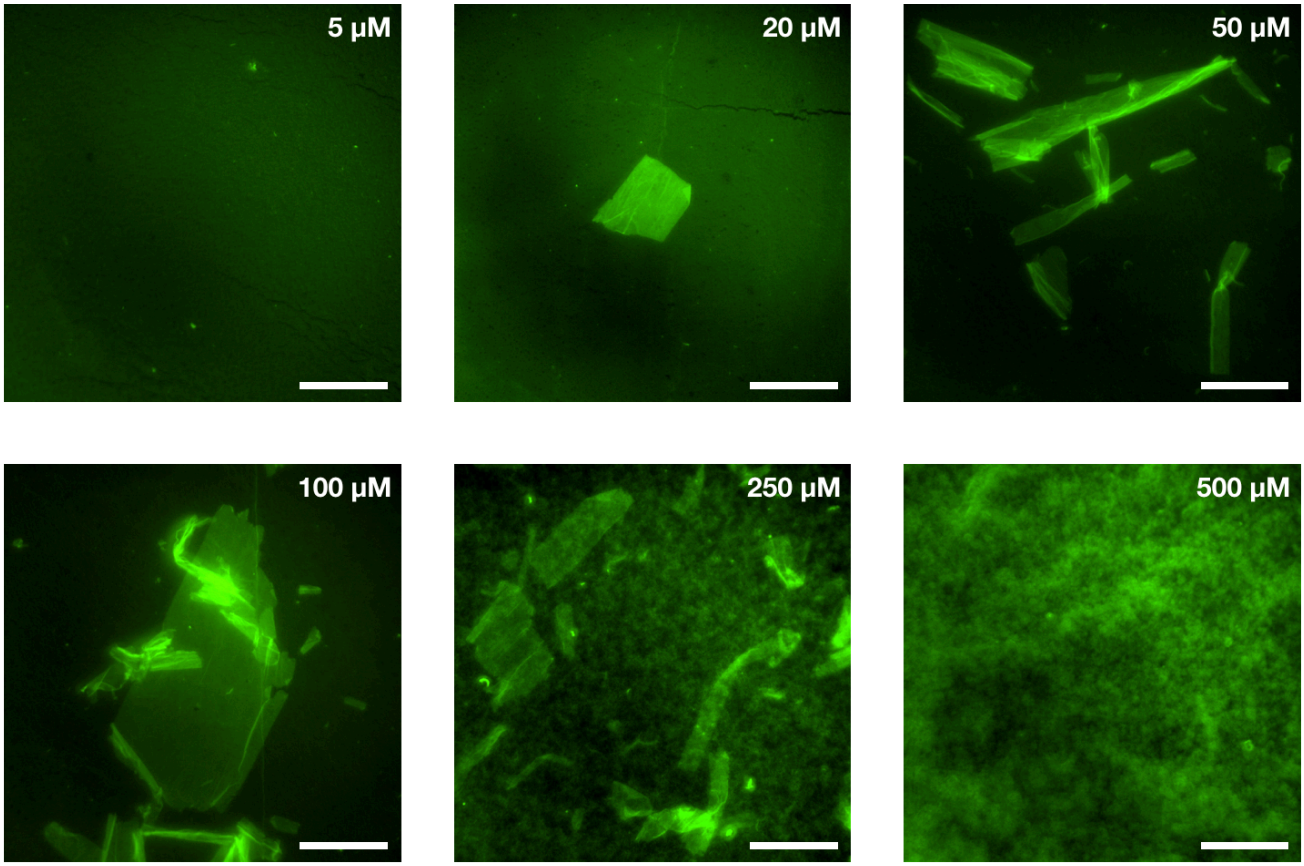

Figure S19 Effect of **CPx** concentration on nanosheet assembly. Epifluorescence micrographs of **CPx** samples prepared at different **CPx** concentrations (5-500 µM, see insets). Scale bars = 50 µm.

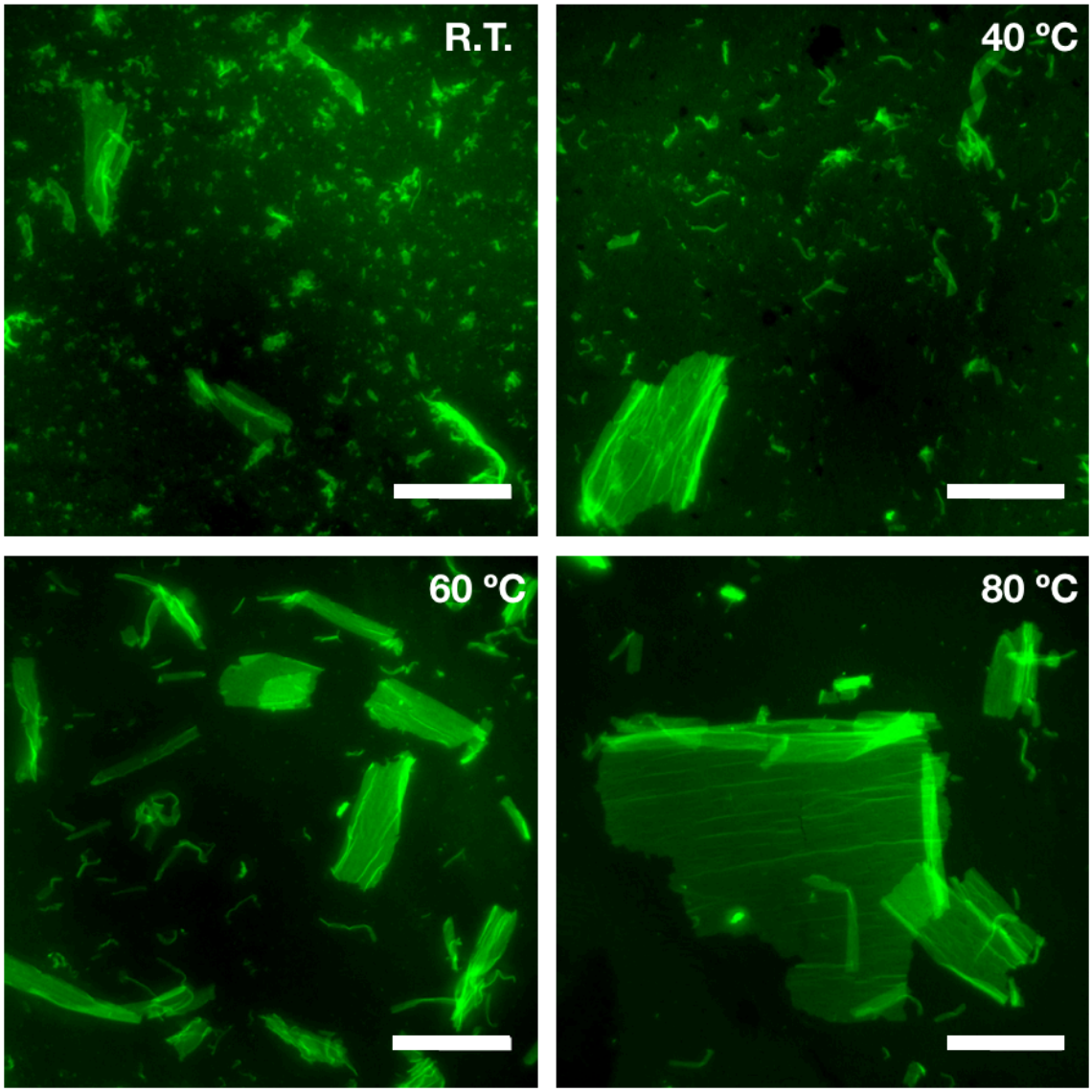

Figure S20 Effect of temperature on nanosheet assembly. Epifluorescence micrographs of **CPx** samples (100 µM) annealed at different temperatures (see insets). R.T. = Room temperature. Scale bars = 50 µm.

15. Atomic force microscopy (AFM) of CPx nanosheets at pH 2.8

Nanosheet height at pH 2.8 (Figure S22) matches that observed at pH 7.4 (Figure 4a).

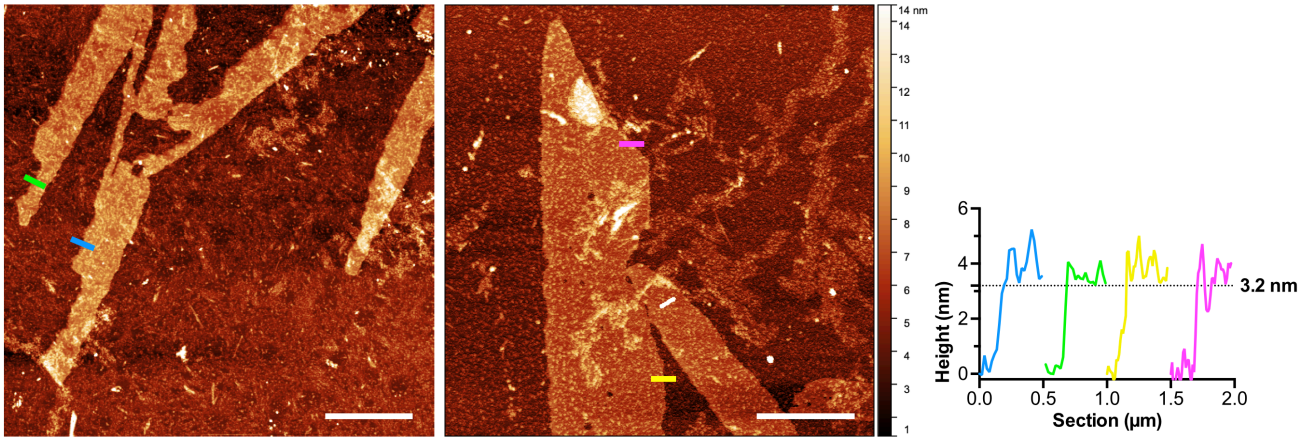

Figure S21 Atomic force micrographs and height profiles of **CPx** nanosheets annealed (i. 80°C /1.5 h; ii. R.T./1 h) at pH 2.8. Scale bars = 2 µm.

16. Dynamic behaviour of CPx nanosheets in response to pH and temperature

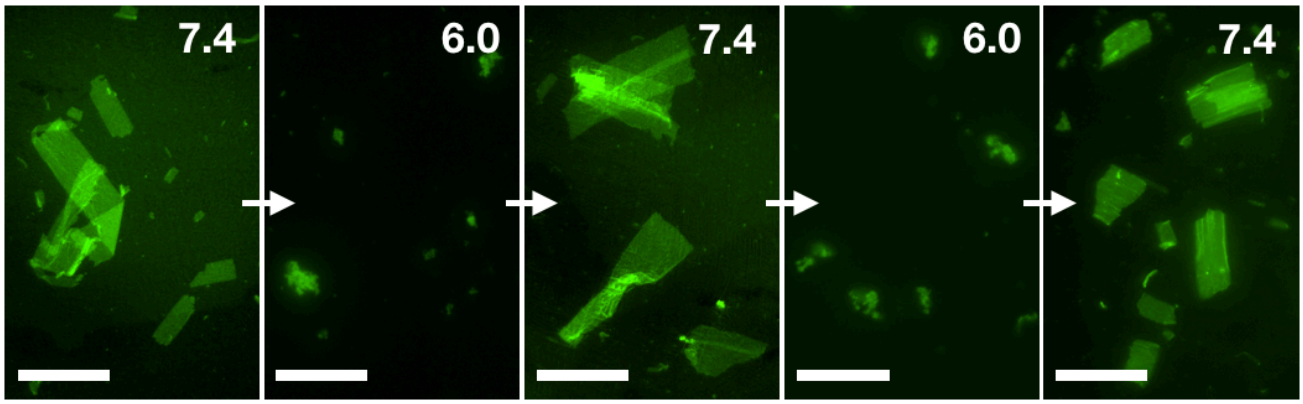

Figure S22 Epifluorescence micrographs of **CPx** solutions (100 µM) sequentially adjusted between pH 6.0 and 7.4. All samples underwent a heating-cooling cycle (i. 80°C /1.5 h; ii. R.T./1 h) before imaging. Scale bars = 50 µm.

17. FT-IR analysis of CPx nanosheets

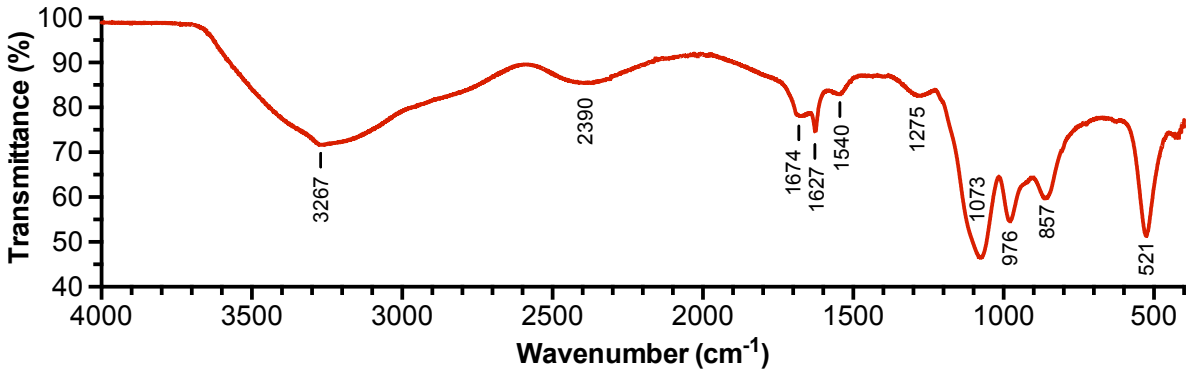

Figure S23 FT-IR spectrum of **CPx** nanosheets. Bands corresponding to the H-bonded backbones of cyclic peptides as β-sheets are indicated with a black line between the spectrum and their wavenumber. The sample was drop-cast (5x 10 µL) and dried on the ATR crystal for analysis.

18. Circular dichroism (CD) analysis of CPx nanosheets

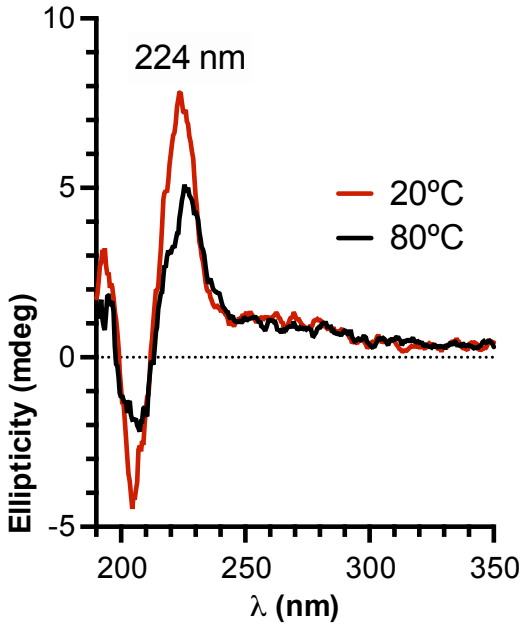

Figure S24 Circular dichroism (CD) spectrum of **CPx** nanosheets (100 µM) at a pH of 7.4 recorded at 20°C and 80°C.

19. Imaging of peptide controls (CPxAla, CPx-Glu and CPx-His)

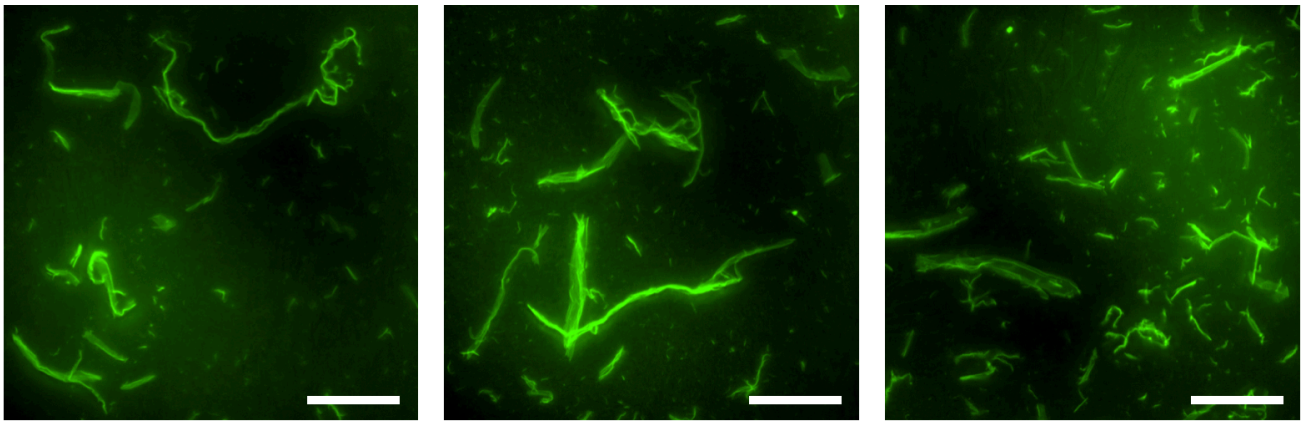

Figure S25 Epifluorescence micrographs of **CPxAla** solutions (100 µM) prepared in 20 mM phosphate buffer at pH 7.4. Samples underwent a heating-cooling cycle (i. 80°C /1.5 h; ii. R.T./1 h) before imaging. Scale bars = 50 µm.

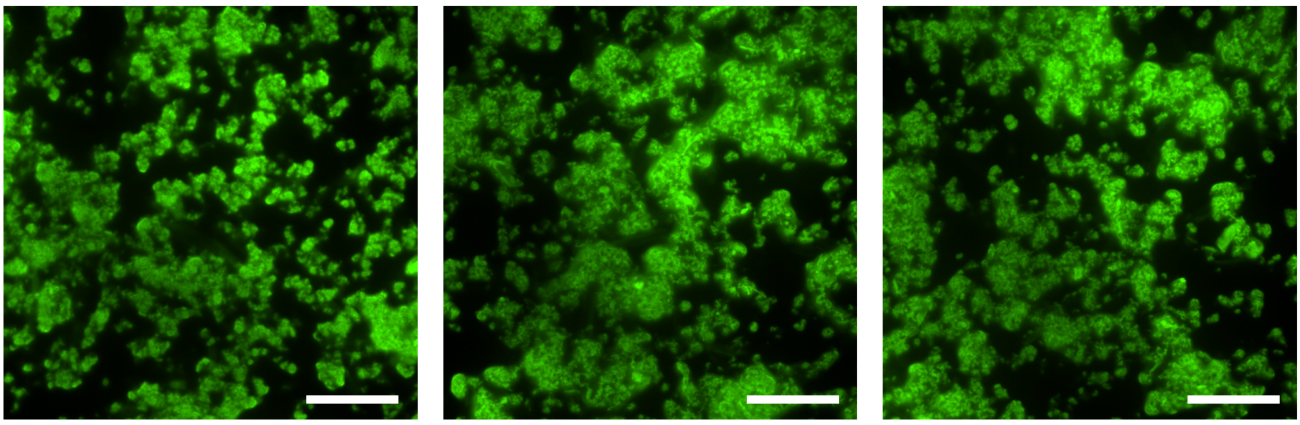

Figure S26 Epifluorescence micrographs of **CPx-Glu** solutions (100 µM) prepared in 20 mM phosphate buffer at pH 7.4. Samples underwent a heating-cooling cycle (i. 80°C /1.5 h; ii. R.T./1 h) before imaging. Scale bars = 50 µm.

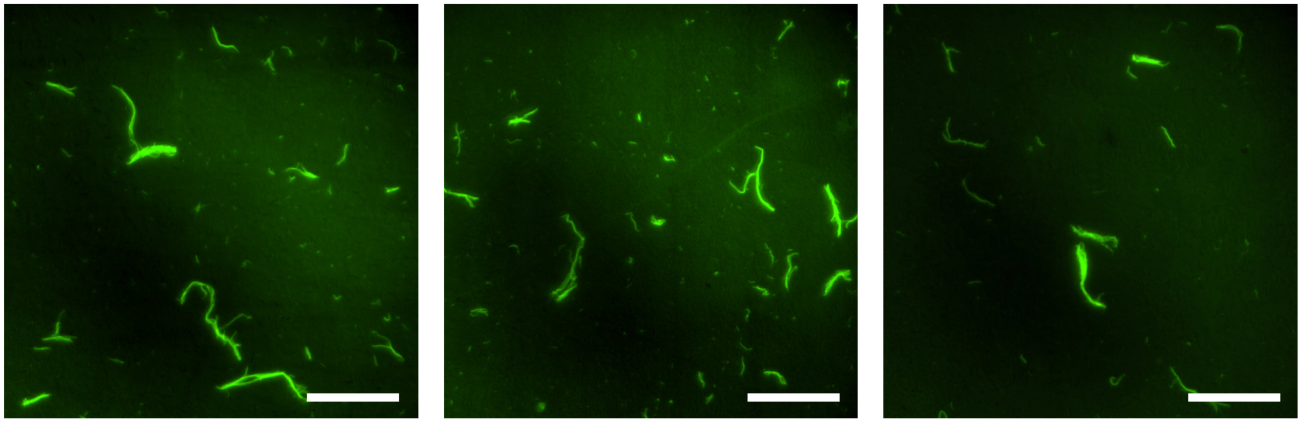

Figure S27 Epifluorescence micrographs of **CPx-His** solutions (100 µM) prepared in 20 mM phosphate buffer at pH 7.4. Samples underwent a heating-cooling cycle (i. 80°C /1.5 h; ii. R.T./1 h) before imaging. Scale bars = 50 µm.